Development 136, 1963-1975 (2009) doi:10.1242/dev.022426

Selective plane illumination microscopy techniques in developmental biology

Jan Huisken* and Didier Y. R. Stainier

Selective plane illumination microscopy (SPIM) and other fluorescence microscopy techniques in which a focused sheet of light serves to illuminate the sample have become increasingly popular in developmental studies. Fluorescence light-sheet microscopy bridges the gap in image quality between fluorescence stereomicroscopy and high-resolution imaging of fixed tissue sections. In addition, high depth penetration, low bleaching and high acquisition speeds make light-sheet microscopy ideally suited for extended time-lapse experiments in live embryos. This review compares the benefits and challenges of light-sheet microscopy with established fluorescence microscopy techniques such as confocal microscopy and discusses the different implementations and applications of this easily adaptable technology.

Introduction

In many commonly used model systems a variety of transgenic animals can be generated in which fluorescent proteins label individual cells, particular tissues or whole embryos. Such fluorescent transgenic organisms offer the opportunity to visualize cell and tissue behavior during developmental processes at high resolution (see Glossary in Box 1) and, in real time, observations that might shed light on the dynamics that are involved in shaping a complex organism. This endeavor, however, is often limited by the technical constraints of the imaging apparatus.

In vivo imaging can potentially capture quantitative data at single-cell resolution. When this imaging is performed noninvasively on intact, fully functioning organisms, time-lapse microscopy allows the study of development over time. Ultimately, one goal is to image and track every single cell in a developing tissue, to digitize all these data from several embryos and to fuse this information into a 'model embryo'. Whereas fluorescence microscopy techniques have become increasingly powerful in terms of resolution, speed and penetration, they most often do so only in thin and transparent samples. The size and opacity of whole embryos, which are often a few millimeters in size, make it especially challenging to achieve single-cell resolution (of ~10 μm) several hundred microns deep inside intact embryos.

In addition, the resolution that can be achieved in live specimens is generally lower than that in fixed specimens because of the size of the sample, the scattering (see Glossary in Box 1) of intact and opaque tissue, pigmentation in untreated animals, the movement of living organs (skeletal muscles, gut, heart, blood, eyes, etc.) and the need to keep the sample under physiologically sustainable conditions. Because of these limitations, scientists are frequently forced to fix and section their samples, even though many of the highly dynamic processes that occur during development can only be studied in full detail in the intact, living embryo. If experimental measurements are to represent normal development, living organisms should not be squeezed between sheets of glass or be exposed to vast amounts of laser light, which frequently results in photo-bleaching (see Glossary in Box 1), photo-damage, or heating.

Several recently introduced imaging techniques that provide ultra-high resolution in fixed and cleared tissue (see Glossary in Box 1), or in thin cultured cells, are incompatible with large scattering objects and are thus unsuitable for live imaging. This incompatibility is especially true for techniques that rely on the interference or overlap of two laser beams or on the projection of patterns (such as structured illumination, 4Pi or stimulated emission depletion) (for a review, see Hell, 2007). The scattering in live tissue can destroy the intended pattern, which would result in aberrated images.

Selective plane illumination microscopy (SPIM) is a fluorescence microscopy technique that uses a focused light-sheet (see Glossary in Box 1) to illuminate the specimen from the side. Techniques like SPIM, generally called light-sheet microscopy methods, are becoming increasingly popular because they achieve excellent resolution at high penetration depths (see Glossary in Box 1) while being minimally invasive at the same time (e.g. Huisken et al., 2004; Verveer et al., 2007). In this review, we will discuss the potential of SPIM and that of related light-sheet-based microscopy techniques, and their applications to developmental biology. We begin by contrasting light-sheet microscopy with classical approaches to imaging three-dimensional (3D) samples, and then consider the concept behind SPIM, the setup required for its use and how it can be adapted for specific applications. Finally, we address the issue of appropriate specimen preparation and provide examples for some of the many applications of light-sheet microscopy to research in developmental biology.

Optical sectioning

The 3D extent of a fixed sample can be imaged at high resolution by physically sectioning it. The achievable resolution is determined by the thickness of the sections and the imaging modality that is used to image them. As precise cutting, mounting and imaging of these sections take considerable amounts of effort, time constraints usually limit the achievable resolution and the size of the imaged volume. Further challenges lie in the registration of the individual datasets and in the segmentation and visualization of the resulting data. Semi-automated techniques, such as serial blockface imaging, have been employed to image whole embryos by light microscopy (e.g. Ewald et al., 2002; Weninger et al., 2006) and tissues by electron microscopy (Denk and Horstmann, 2004). Despite these advances, however, physical sectioning precludes studies in live samples by its very nature. Hence, a prerequisite for 3D in vivo fluorescence microscopy is optical sectioning.

Optical sectioning, in contrast to physical sectioning, allows the sample to be left intact and alive. The images acquired are optically confined to single slices of the sample with a well-defined thickness. The resulting images show single sections of the sample, free of the

Department of Biochemistry and Biophysics, and Cardiovascular Research Institute, University of California, San Francisco, CA 94158, USA.

*Author for correspondence (e-mail: jan.huisken@ucsf.edu)

Box 1. Glossary

Clearing. Chemical process to render fixed samples translucent, a sample preparation step commonly used in optical projection tomography (OPT) and ultramicroscopy.

Dichroic mirror. Mirror that selectively reflects one or more parts of the light spectrum while transmitting the rest of the spectrum; commonly used to split the fluorescence from multiple fluorophores.

Electron multiplication (EM)-CCD camera. Quantitative digital camera capable of detecting single photons. Weak signals are multiplied before the noise-prone amplification step. Their sensitivity makes EM-CCD cameras ideal for high-speed and low-light fluorescence microscopy.

Epifluorescence microscopy. The simplest mode of fluorescence microscopy, in which the whole sample is illuminated and the image is observed directly through a single objective lens.

Field of view (FOV). Area 'seen' by the microscope; depends on the magnification of the optics and the size of the camera chip. In light-sheet microscopy, the light-sheet thickness is optimized to uniformly cover the full FOV.

Fluorophore. Molecule in which the absorption of a photon triggers the emission of a photon with a longer wavelength, making it visible in a fluorescence microscope. Biological tissues and proteins are commonly labeled with fluorophores through immunostaining or transgenesis.

Gain. Amplification of the signal from a camera or photomultiplier to increase image brightness; increased gain is generally accompanied by noise (see EM-CCD camera).

Isotropic. Uniform in all directions. Isotropic resolution in microscopy is especially desirable for 3D reconstructions and quantitative analysis.

Light-sheet. A thin sheet of laser light used to selectively illuminate the sample in the focal plane of the detection system.

Numerical aperture (NA). Dimensionless measure of the ability of an optical system to gather or emit light. It is defined as the product of the medium's refractive index n and the sine of the half angle of the maximum cone of light that can enter or exit the lens. The lateral and axial resolution of an objective lens are inversely proportional to the NA and the NA^2, respectively.

Penetration depth. Depth to which a satisfying image quality can be achieved; depends on the transparency of the sample and the imaging modality used.

Photo-bleaching. Process whereby a molecule is rendered nonfluorescent. Almost all fluorophores fade during light exposure.

Photo-conversion. Several fluorophores change color upon irradiation with short wavelengths (for example Kaede, Dendra, Dronpa and Eos). Single cells can be targeted and photo-converted from one color to another to facilitate their tracking.

Photomultiplier. Glass vacuum tube in which a cascade of electrons is induced by the arrival of a single photon; fast, single channel detector commonly used in confocal microscopy.

Positioning stages. Micromotors to control the position of the sample. Three motors can move the sample in all three dimensions (x, y and z). Three-dimensional (3D) stacks of images are acquired by stepwise movement along the axis of the detection lens. In SPIM, the sample can also be turned by a fourth motor.

Raster imaging. Process in which the final image is built up piece by piece through the sequential illumination (and detection) of small areas (point or lines); required in microscopes that image only a fraction of the image at a time, such as confocal and multi-photon microscopes.

Resolution. Smallest distance between two points in a specimen that can still be distinguished as two separate entities. Theoretically only dependent on the NA and the wavelength of light used to image the object. In practice, the achievable resolution also depends on additional parameters such as contrast, noise and sampling. In single-lens microscopy, the axial resolution along the axis of the detection objective is always worse than the lateral resolution.

Saturation. Fluorescence does not increase linearly with excitation intensity when the light is so intense that a significant fraction of dye molecules in the illuminated area is already in the excited state. The final image is hence not solely dependent on the dye concentration.

Scan mirrors. Rapidly moving mirrors required in point or line scanning microscopes to sequentially illuminate the whole area of interest.

Scattering. Non-uniformities in the sample cause the light to deviate from its straight path. The resulting blur in the illumination and in the detection process limits the penetration depth of most microscopes.

Spherical aberrations. A spherically aberrated lens focuses axial and peripheral rays to different points, thus blurring the image of a point source of light; induced by refractive index mismatch, for example.

Tomography. An imaging approach in which, after gathering projection data from multiple directions, the three-dimensional object is reconstructed in the computer, for example by backprojection.

blur generated by the rest of the sample. Optical sectioning in fluorescence microscopy can be achieved in three different ways: (1) image processing, for example deconvolution; (2) illuminating the (whole) sample and limiting the detection to the desired volume; or (3) restricting the excitation to the plane of interest and detecting all the fluorescence from the sample. We will discuss these approaches in turn.

Optical sectioning by deconvolution (e.g. McNally et al., 1999) does not require any special microscope hardware and can be performed on data from commonly used widefield microscopes with motorized positioning stages (see Glossary in Box 1). 3D stacks of images are acquired and processed with one of the various deconvolution algorithms, which allow the in-focus information from each plane to be extracted while the blurry contribution from adjacent planes is suppressed. Despite the need for computationally intense post-processing, the actual image acquisition can be performed at high speed. Backprojection, another image processing technique, produces optically sectioned images from data acquired with tomographic imaging techniques, such as optical projection tomography (OPT; see Glossary in Box 1) (Sharpe et al., 2002). The tomographic dataset consists of projections acquired at different orientations of the sample and is processed to yield a 3D image of the sample. A drawback of these image processing approaches is that the user has to wait for the processing to finish and cannot see the optical sections in real time. In addition, deconvolution relies on a number of assumptions about the optical properties of the sample and about the performance of the microscope (e.g. linearity and space invariance), which in less than ideal conditions (e.g. due to the presence of noise or optical imperfections) can lead to artifacts.

The second approach to optical sectioning, in which the whole sample is illuminated and the detection is limited to the desired volume, is realized in laser scanning confocal microscopy (LSCM) (Pawley, 2006), whereby the focal spot of a laser is scanned across the sample to build up an image pixel by pixel. Optical sectioning is achieved in the detection path during the scan, where the fluorescence light that generates each pixel is focused onto a pinhole. The pinhole discriminates out-of-focus light, and its adjustable size determines the thickness of the section that is imaged. This rejection of out-of-focus light, however, can only be efficiently achieved in non-scattering tissue. For thick, scattering samples, the penetration depth of a confocal microscope is limited and often becomes apparent as a drop in image brightness with increasing depth. Another limitation of LSCM is the inherently slow raster imaging (see Glossary in Box 1). A higher number of pixels translates into longer acquisition times or shorter time spent per pixel (the so-called pixel dwell time); the shorter the time spent collecting photons, the higher the detector gain (see

Glossary in Box 1) or the higher the laser power needs to be, which can lead to noise and fluorophore saturation (see Glossary in Box 1), respectively. The excitation light is not axially confined, i.e. the whole depth of the sample is exposed to the fluorescence excitation light, and hence the sample is potentially bleached or damaged even when only a single image is acquired. These negative effects scale with the number of planes that are acquired: In a stack of 100 planes, the last plane imaged has already been exposed 99 times. In addition, the efficiency of the photomultipliers (see Glossary in Box 1) of a confocal microscope is approximately two to three times worse than the efficiency of modern cameras. Nevertheless, the confocal microscope is a routine instrument found in many laboratories. Its optical sectioning properties make it ideally suited for the 3D imaging of tissue sections of thickness in the order of 100 μm and for time-lapse experiments of tissue dynamics near the surface of relatively transparent embryos, such as those of the zebrafish (e.g. Haas and Gilmour, 2006; Rembold et al., 2006).

In the third approach to optical sectioning, fluorescence is excited only where it is needed, which leaves the remainder of the sample unexposed and therefore free of photo-bleaching and -damage. This approach is taken in multi-photon microscopy and in fluorescence light-sheet microscopy in two very different ways. In multi-photon microscopy, a tightly focused high-intensity infrared laser pulse penetrates the sample and excites fluorescence only in a small volume in the focus of the beam. This nonlinear multi-photon excitation prevents excitation outside of the focal plane. The use of longer wavelengths employed for multi-photon microscopy increases the penetration depth (up to 700 μm) (Helmchen and Denk, 2005) but reduces the resolution compared with single-photon confocal microscopy. In addition, high power laser pulses are required, and over time the whole sample can suffer from the detrimental effects of light, such as heating, photo-bleaching and photo-damage. Absorption of infrared light can severely damage specimens, one of the reasons why zebrafish embryos are routinely treated to be pigment-free when imaged with multi-photon microscopy (e.g. Kamei and Weinstein, 2005). In light-sheet microscopy, however, a different approach is taken to selectively illuminate the area of interest while at the same time preventing the sample from damage, as discussed in the following section.

Light-sheet fluorescence microscopy: concept and components

The idea behind SPIM and other light-sheet-based microscopy techniques is to illuminate the sample from the side in a well-defined volume around the focal plane of the detection optics (see Box 2). Even though there are many different implementations of this idea (see below and Table 1), the common general principles remain the same and are illustrated in Fig. 1. The following sections describe the illumination, detection and photo-manipulation units in SPIM and illustrate the major benefits of this approach, such as optical sectioning, reduced photo-bleaching and high-speed acquisition (see Box 3 for a historical perspective of the concept).

Illumination

The ideal scenario, a perfectly thin optical section, would be obtained if a sheet of light illuminated only the focal plane of the detection objective. Preferably, this sheet should be as thin as possible and uniform across the field of view (see Glossary in Box 1). However, diffraction sets a limit on how thin the illuminated volume can be. In SPIM, a currently widely adopted light-sheet microscope system, cylindrical optics are used to create a sheet of light of varying thickness. The light converges towards the sample and diverges away from it. The waist of the light-sheet is positioned in the center of the field of view. The dimensions of the light-sheet can be adapted to different sample sizes: for smaller samples (20-100 μm), the light-sheet can be made very thin (~1 μm); whereas for larger samples (1-5 mm), the sheet has to be thicker (~5-10 μm) to remain relatively uniform across the field of view (Engelbrecht and Stelzer, 2006).

Alternatively, the sheet of light can be generated by focusing a laser beam to a single line and by rapidly scanning it up and down during the exposure time. This concept was recently introduced as digital scanned laser light-sheet fluorescence microscopy (DSLM) (Keller et al., 2008). The benefit of this technique is the uniformity of the light-sheet intensity profile and the ability to control its height through computer-controlled scan mirrors (see Glossary in Box 1). In other light-sheet-based techniques, the laser light is expanded and cropped with apertures to cover the field of view of the detection lens, resulting in a less uniform intensity profile. Owing to the sequential line illumination in DSLM, the beam illuminates only a fraction of the final image at any one time. Therefore, the sample is typically exposed to a local light intensity that is ~300 times higher than in SPIM in order

Box 2. SPIM basics

The basic principle of SPIM is to illuminate the sample from the side in a well-defined volume around the focal plane of the detection optics (Fig. 1). The illumination and the detection path are distinct and perpendicular to each other. The illuminated plane is aligned to coincide with the focal plane of the detection objective. Hence, the illumination light can be shaped and positioned independently of the detection optics and thus does not share the same constraints, such as numerical aperture and working distance. The sample is placed at the intersection of the illumination and the detection axes. The illumination sheet excites fluorescence in the sample, which is collected by the detection optics and imaged onto a camera. For a single 2D image, no scanning is necessary. To image the 3D extent of the sample, the sample is moved along the detection axis in a stepwise fashion, and a stack of images is acquired.

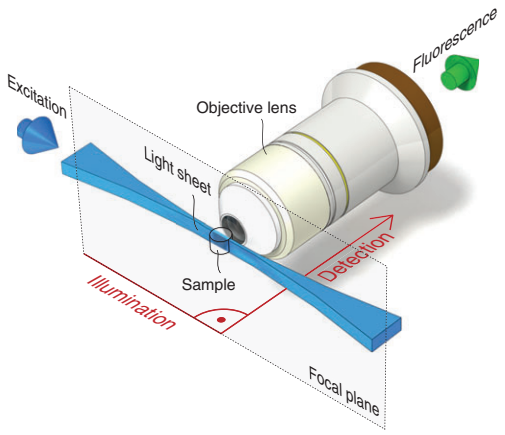

Fig. 1. The concept behind fluorescence light-sheet microscopy. In light-sheet microscopy, fluorescence excitation (blue arrow) and detection (green arrow) are split into two distinct optical paths. The illumination axis is orthogonal to the detection axis. A microscope objective lens and common widefield optics are used to image the sample onto a camera (not shown). The illumination optics are designed to illuminate a very thin volume around the focal plane of the detection objective. Many different implementations of this principle exist, however, the most common one is the generation of a sheet of laser light that illuminates the sample in the focal plane from one side.

Table 1. Overview of fluorescence light-sheet techniques in comparison with epifluorescence, confocal and two-photon microscopy

Technique	Unique features	Advantages	Disadvantages	Ideal application	References
Fluorescence microscopy					
Epifluorescence microscopy	Uniform illumination of the sample	Easy to use, low cost	No optical sectioning	Screening, thin sections	
Confocal microscopy	Point illumination (laser focus) and point detection (pinhole)	Optical sectioning, improved resolution ($\sqrt{2}$)	Slow scanning, low penetration	Medium-thick sections, surface of embryos	Pawley, 2006
Two-photon microscopy	True 3D imaging, infrared laser	Low scattering, excellent penetration, reduced bleaching	Slow scanning, low resolution, high cost, high power beam	Deep penetration in scattering tissue	Helmchen and Denk, 2005
Fluorescence light-sheet microscopy					
Orthogonal-plane fluorescence optical sectioning (OPFOS)	Single-sided light-sheet illumination	Optical sectioning	Shadows, stripes	Fluorescently stained samples	Voie et al., 1993
High-resolution orthogonal-plane fluorescence optical sectioning (HROPFOS)	Like OPFOS, light-sheet translated	Thin light-sheet of constant thickness	Slow, shadows, stripes	Like OPFOS	Buytaert and Dirckx, 2007
3D light scanning macrography	Extended depth of field	Large samples	Only surface	Surface scanning of flies	Huber et al., 2001
Thin light-sheet microscope (TLSM)	Light-sheet illuminates tank of medium from the side	Improved contrast in aqueous suspensions	Low resolution	Aquatic microbes	Fuchs et al., 2002
Selective plane illumination microscopy (SPIM)	Single-sided light-sheet illumination, sample rotation about vertical axis	Fast acquisition, low photo-bleaching, good penetration, MVR	Shadows, stripes	Extended time-lapse imaging of millimetre-sized embryos, high speed movies	Huisken et al., 2004
Objective coupled planar illumination (OCPI) microscopy	Single-sided light-sheet illumination, attached to detection lens	Fast stack acquisition, no sample movement, conventional sample	Shadows, stripes	Conventionally prepared samples, fast 3D imaging	Holekamp et al., 2008
Ultramicroscopy	Dual-sided light-sheet illumination, upright detection path	Sealed chamber with clearing solution	No index-matched optics, stripes	Large fixed and cleared specimens	Dodt et al., 2007
Digital scanned laser light-sheet fluorescence microscopy (DSLM)	Like SPIM, light-sheet generated by beam scanning	Like SPIM, uniform, adjustable light-sheet	Like SPIM	Like SPIM	Keller et al., 2008
Multidirectional SPIM (mSPIM)	Like SPIM, pivoting light-sheet, two alternating illumination arms	Like SPIM, reduced stripes, reduced shading	Space constraints	Like SPIM, especially scattering and absorbing tissue	Huisken and Stainier, 2007
Highly inclined and laminated optical sheet (HILO) microscopy	Single lens for oblique light-sheet illumination and detection	Single lens	Very narrow FOV	Single cell microscopy close to the coverslip	Tokunaga et al., 2008
Oblique plane microscopy (OPM)	Like HILO, matching, tilted image plane	Like HILO, extended FOV	Extensive optics	Like HILO	Dunsby, 2008

to achieve the same fluorescence yield across the final image in the same amount of time (Keller et al., 2008). In SPIM, the light-sheet illuminates the entire object plane at once and can therefore be triggered for arbitrary time periods. For example, in SPIM, the illumination time can be set to less than 1 ms to 'freeze' the rapid motion of the heart and the flow of red blood cells (Scherz et al., 2008). In DSLM, the light-sheet can also be spatially structured to further reduce out-of-focus light in transparent samples, as previously demonstrated in a SPIM setup (Breuninger et al., 2007). In this technique, the sample is illuminated with a periodic and symmetric pattern. Multiple images are taken at different positions of the pattern, and an image with improved contrast is calculated. However, this approach is likely to be unsuitable for imaging light-scattering tissues, as this periodic illumination pattern would be disturbed by the scatter,

Box 3. Early history of light-sheet-based techniques

Light-sheet-based techniques in microscopy can be roughly divided into three categories: single particle, extended depth of field and fluorescence microscopy.

The earliest instrument we found that employs the principle of light-sheet microscopy is the work of Siedentopf (Siedentopf and Zsigmondy, 1902), who used a light-sheet to observe gold particles in glasses. The light-sheet allows the observer to focus on a few particles in an ensemble of many particles. The use of a light-sheet instead of a uniform illumination dramatically increases the signal-to-noise ratio and makes visible single particles, which would otherwise be indistinguishable from the rest. Modern applications of this idea include the thin light-sheet microscope (TLSM) for visualizing aquatic microbes (Fuchs et al., 2002) and the single particle tracking microscope (Ritter et al., 2008).

Later, light-sheets were used for extended depth of field photography (Zampol, 1960), deep focus microscopy (Simon, 1965; McLachlan, 1968) and 3D light scanning macrography (Huber et al., 2001). In this application, a macroscopic object is slowly moved through a light-sheet, while a camera that is focused on the illuminated plane is continuously exposed. The result is a photo of the object in which every portion is in focus.

It was not until 1993 that fluorescently labeled macroscopic biological samples were illuminated with light-sheets to achieve optical sectioning: orthogonal-plane fluorescence optical sectioning (OPFOS) (Voie et al., 1993) was primarily developed to image the internal architecture of the cochlea (Voie, 2002) and was later modified to a high-resolution version (HROPFOS) (Buytaert and Dirckx, 2007).

and the algorithm employed to generate the final image would subsequently remove the corresponding fluorescence signal from the scattering parts of the sample.

The thickness of the light-sheet determines the depth of the optical section viewed by the camera, which is usually 1-10 μm, depending on the field of view (see Glossary in Box 1). In many cases, it also defines the axial resolution of the system, i.e. the resolution along the optical axis of the detection lens. Most applications in developmental biology require long working distance objective lenses with a relatively low numerical aperture (NA; see Glossary in Box 1). Such lenses have sufficient lateral resolution but suffer from poor axial resolution in classical widefield microscopes. In light-sheet microscopy, however, the light-sheet defines the volume that is illuminated and therefore 'seen' by the camera, which increases the axial resolution significantly. The axial resolution in SPIM is theoretically better than that of epifluorescence microscopy (see Glossary in Box 1) and two-photon microscopy and, in many cases (NA<0.8), it is better than the axial resolution in confocal microscopy (Engelbrecht and Stelzer, 2006).

Theoretically, the lateral resolution in light-sheet microscopy is equivalent to the lateral resolution in epifluorescence microscopy, which is given by the NA of the objective lens and the wavelength of the fluorophore. In practice, however, the lateral resolution in light-sheet microscopy is often even better because of improved contrast due to the optical sectioning. In SPIM, fine structures are resolved that would be obscured by the out-of-focus haze in epifluorescence microscopy.

Fig. 2 illustrates the lateral illumination in light-sheet microscopy and its advantage over LSCM. As the laser beam scans across the sample in confocal microscopy, the whole sample gets exposed to the light (Fig. 2A). The pinhole in the detection unit rejects out-of-focus light and confines the detection volume to a thin slice (Fig. 2B). By contrast, the light-sheet illumination exposes only a narrow volume around the focal plane and leaves the rest of the sample unaffected (Fig. 2C). A charge-coupled device (CCD) camera collects all the fluorescence from the sample at once without the need for raster scanning (Fig. 2D). This design makes data acquisition in light-sheet microscopy extremely fast and efficient in comparison with confocal and other scanning microscopes.

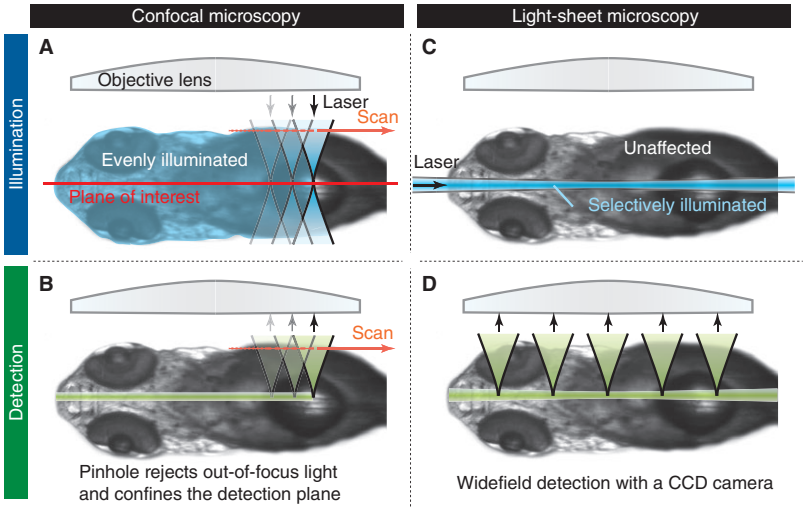

Fig. 2. Advantages of light-sheet microscopy compared with confocal microscopy. Light-sheet microscopy features faster acquisition and less photo-bleaching than confocal microscopy. To illustrate the difference between laser scanning confocal microscopy (LSCM; **A**,**B**) and light-sheet microscopy (**C**,**D**), the processes of illumination (A,C) and detection (B,D) are split. (A,B) In LSCM, a tightly focused laser beam is scanned across the sample (A), thereby exposing the sample to high-intensity light not only in the plane of interest, but also above and below. (B) A pinhole rejects much of the excited fluorescence and confines the image to the plane of interest. (C,D) In light-sheet microscopy, a light-sheet from the side (C), which overlaps with the plane of interest, illuminates the sample in a thin slice. Photo-bleaching is thereby considerably reduced. (D) All the fluorescence is collected and imaged onto a CCD camera. Such widefield detection is fast and benefits from modern CCD technology.

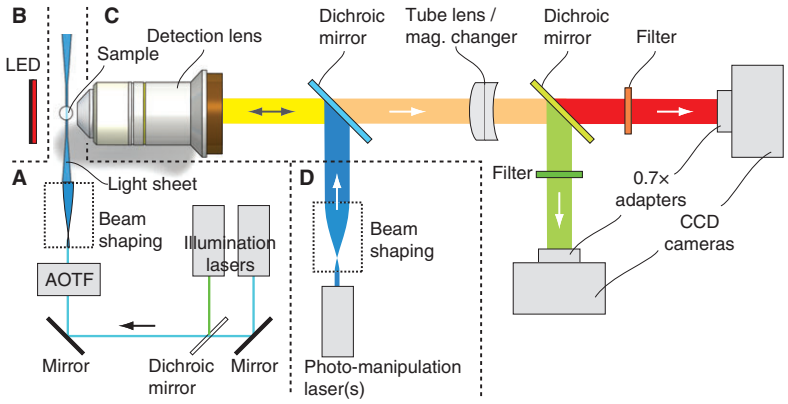

Fig. 3. Typical SPIM components (not to scale). A typical SPIM setup consists of an illumination, a detection and (optionally) a photo-manipulation unit. (**A**) Fluorescence illumination: the light from one or more lasers is collected and focused by optics to become a sheet of light in the focal plane of the detection lens. An acousto-optic tunable filter (AOTF) is used to precisely control the exposure of the sample. (**B**) Transmission light: a red light emitting diode (LED) array provides uniform transmission light without bleaching the sample. (**C**) Fluorescence detection: the fluorescence from the sample is imaged onto one or more cameras. As shown here, two cameras are used to simultaneously image green and red fluorescence split by a dichroic mirror. The magnification of the system is given by the objective, the camera adapters and the optional magnification changer. (**D**) Photo-manipulation: laser light, which can be used to selectively photo-bleach, photo-convert or microdissect, is directed through the detection lens and focused onto the sample. Either the beam or the sample is moved to irradiate multiple points or areas in the sample.

In speed-demanding applications (for example cardiac imaging), frame rates of 30 to 200 frames per second (fps) at sufficient spatial resolution (1000 to 200 lines, respectively) can be achieved in light-sheet microscopy in combination with fast and sensitive cameras such as electron multiplication CCD (EMCCD) cameras (see Glossary in Box 1). Confocal microscopes achieve such speeds only in multi-point or in line-scanning mode, both of which reduce the effectiveness of the optical sectioning. Ultimately, the speed of image acquisition in LSCM is limited by the saturation of fluorophores that occurs at high scanning speeds, which necessitates high light intensities and short dwell times. Moreover, images of rapidly moving samples show artifacts when acquired line-by-line because of the inherent delay between adjacent lines across the whole image.

High data acquisition speeds are also beneficial in multi-dimensional recordings, in which thousands of images in different colors are acquired over the course of several hours. In light-sheet microscopy, stacks of images can be recorded in a few seconds, allowing high repetition rates in time-lapse recordings (Keller et al., 2008). This potential can be exploited in multi-sample recordings, in which several embryos are monitored as part of a time-lapse recording (see below).

Similar to the common setups for LSCM, a variety of lasers are used in light-sheet microscopy to excite fluorescence in the sample. The most commonly used laser lines have wavelengths of 488 nm [for example for green fluorescent protein (GFP)] and 561 nm or 568 nm (for example for the fluorophores mCherry and DsRed). In SPIM, the light from all lasers is combined into a single beam and shaped by optics into a light-sheet (Fig. 3) (for details, see Huisken et al., 2004; Huisken and Stainier, 2007). An acousto-optic tunable filter (AOTF) is often used to precisely control the wavelength, power and timing of the illumination. Brightfield illumination is a useful additional feature in light-sheet microscopy to facilitate sample alignment and to inspect the constitution of the specimen before and during an experiment. A light emitting diode (LED) array provides very uniform illumination for this purpose (Fig. 3). Red and infrared LEDs are especially useful as they neither excite fluorescence nor bleach the sample.

Detection system

The detection system in light-sheet microscopy generally consists of a widefield microscope with objective, tube lens and camera (Fig. 3). As light-sheet microscopy is well suited for high-speed microscopy, many applications benefit from a dual camera detection system (Scherz et al., 2008). Multiple fluorophores can be monitored through a dichroic mirror (see Glossary in Box 1), which splits the fluorescence of two spectrally distinct fluorophores, such as GFP and mCherry, and directs it onto two cameras. A computer triggers these cameras at the same time to ensure synchronous image acquisition. A dual camera setup that allows the transmission light from an LED to be recorded simultaneously with a fluorescent marker is useful for monitoring the health of a specimen during time-lapse experiments. Alternatively, a filter wheel in front of a single camera can be used for low-speed multi-color acquisitions. As changing objective lenses can be difficult in some light-sheet techniques that involve water-dipping lenses (see below), a magnification changer is convenient for allowing the flexible adaptation of the magnification to different sample sizes.

Photo-manipulation

Recently, it has become increasingly important in developmental studies to be able to not only image a sample, but also to photo-manipulate the sample using optical tools such as laser cutters or optical tweezers. In fluorescence microscopy, cell and tissue dynamics can be followed by photo-activation, photo-conversion (see Glossary in Box 1) and photo-bleaching. Single or multiple cells can be illuminated to change their appearance for simpler tracking or to physically disrupt cells or subcellular compartments. Photo-manipulation optics can be integrated into SPIM setups (Engelbrecht et al., 2007). As it is usually best to confine the manipulation beam to a small volume and to have precise control over its lateral position, in light-sheet microscopy this beam is focused onto the sample by the detection lens rather than by the cylindrical illumination optics. The beam is expanded and directed into the back aperture of the detection objective lens by a dichroic mirror (Fig. 3) and creates a diffraction-limited spot in the sample. This beam is scanned or the sample is moved to illuminate areas and multiple cells.

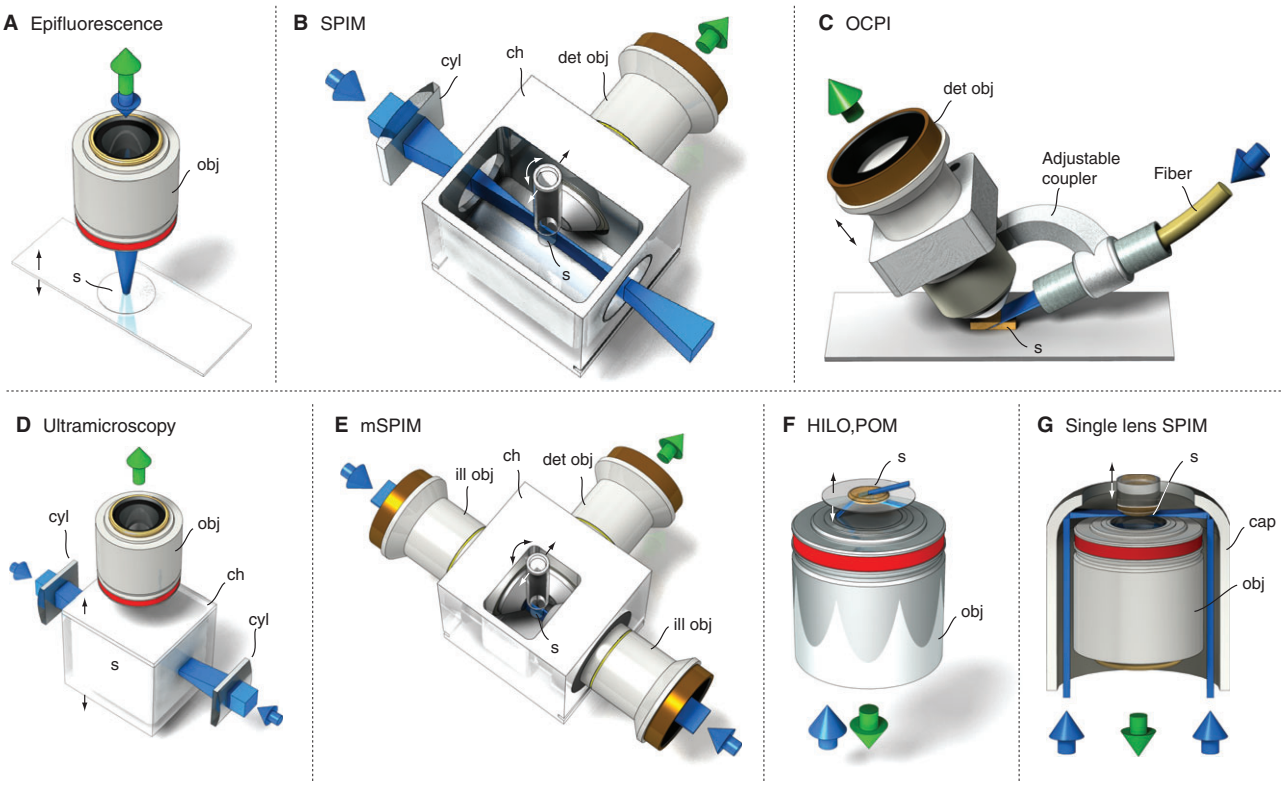

Fig. 4. A comparison of light-sheet microscopy techniques. (**A**) In epifluorescence microscopy, a single objective lens (obj) is used to both illuminate the sample (s) and to collect its fluorescence along the same path. The sample is usually prepared on a glass slide or in a dish. (**B-G**) In light-sheet-based imaging techniques, by contrast, the sample is illuminated from the side by one or two additional beam paths (B-E), through (F) or along (G) the detection lens. (B) In selective plane illumination microscopy (SPIM), the detection lens is horizontally aligned and immersed into a fluid-filled chamber (ch). The sample is embedded in a transparent gel, immersed in the medium and held from the top. A single cylindrical lens (cyl) is used to form the light-sheet inside the chamber. A stack of images is acquired by moving the sample in a stepwise fashion along the detection axis. Optionally, the sample is turned for complementary data acquisition. (C) In objective-coupled planar illumination microscopy (OCPI), the illumination light is delivered through a fiber and focused by optics that are directly attached to the detection lens. A three-dimensional (3D) image stack is rapidly acquired by moving this arrangement, leaving the sample at rest. (D) Ultramicroscopy was developed to image fixed and cleared samples enclosed in a chamber. Two counter-propagating laser beams are focused into a light-sheet by cylindrical lenses and illuminate the sample simultaneously from both sides, thereby providing a more even illumination in clear tissue. (E) In multidirectional SPIM (mSPIM), the sample is illuminated independently from two sides over a range of angles. Shadowing and scattering (a common problem in live, scattering tissue) are thereby reduced. Three water-dipping objective lenses eliminate the need for any chamber windows. (F) In highly inclined and laminated optical sheet (HILO) microscopy, a single lens is used for both illumination and detection; however, the light-sheet is tilted and intersects the focal plane only in the center of the field of view. (G) The concept of an attachment ring to provide light-sheet illumination could be implemented as an add-on to existing microscopes. Blue arrows indicate the direction of illumination, green arrows indicate the direction of detection.

Adapting fluorescence light-sheet microscopy techniques

In conventional epifluorescence microscopy, the excitation light is delivered through the same objective lens that is used to collect the fluorescence (Fig. 4A). In the family of light-sheet microscopy techniques, the excitation light is projected onto the sample from the side, orthogonally to the detection axis. Several different implementations of this idea exist in the literature for numerous applications, which can be roughly divided into three categories: single particle, extended depth of field and fluorescence microscopy (see Box 3).

SPIM is a recent implementation of fluorescence light-sheet microscopy that has found many applications. Using this technique, live fluorescently labeled medaka and *Drosophila* embryos were imaged at previously unmatched spatial (6 μm) and temporal resolution ~500 μm deep inside the sample, and an entire medaka larva was reconstructed from multiple views (Huisken et al., 2004). Fig. 4B shows the core of this first SPIM setup. A cylindrical lens generates the light-sheet inside a buffer-filled chamber. A water-dipping lens is focused onto the light-sheet and detects the fluorescence of the sample in this one plane. Importantly, the optical setup is horizontal and the sample is immersed into the buffer from the top. This vertical sample orientation allows the user to turn the sample to precisely align it in front of the detection lens or to acquire multiple views of the same sample, which are unique features of SPIM.

In SPIM, a stack of images is recorded by moving the sample through the light-sheet in a stepwise fashion. The sample is usually embedded in a soft gel such as agarose, which is not perfectly stiff. Motion-induced vibrations can limit the acquisition speed of 3D datasets. This limitation can be overcome by leaving the sample at rest and by moving the objective lens (including the illumination optics) instead. This design was realized in objective-coupled planar illumination (OCPI) microscopy (Holekamp et al., 2008; Turaga and Holy, 2008). An optical fiber delivers laser light to the illumination

optics, which are directly attached to the objective lens (Fig. 4C). This fixed arrangement of illumination and detection optics can be moved relative to the sample at high speed. Thousands of neurons were imaged in a stack of 50 planes acquired in just 2 seconds with bleaching rates that are approximately 100 times less than in LSCM (Holekamp et al., 2008). The authors used this technique to study fast events in pheromone-sensing neurons in the mouse and reported frame rates of 200 fps, much faster than previously achieved with single- or multi-photon microscopy.

Fixed tissue can be imaged at high resolution in histological sections. 3D reconstructions from many such sections, however, are very laborious and require reliable registration algorithms. Alternatively, the sample can be optically cleared and imaged in toto. A light-sheet technique called ultramicroscopy (Dodt et al., 2007) has been used to image fixed and cleared mouse brains in the arrangement shown in Fig. 4D. Because of the relatively large size of the sample, the excitation light is attenuated as it penetrates the sample. To compensate for this attenuation, two light-sheets are generated, which illuminate the sample from opposing directions. During image acquisition, the sample has to be kept in the clearing solution and enclosed in a glass chamber. The use of air objectives consequently results in less than optimal optical conditions and might lead to spherical aberrations (see Glossary in Box 1). Applications of ultramicroscopy include the imaging of cleared mouse organs and whole-mount embryos, adult *Drosophila* fruit flies and other fixed tissues a few millimeters in size (Becker et al., 2008). An alternative imaging technique, optical projection tomography (OPT) (Sharpe et al., 2002), has also been shown to give excellent results for similarly prepared, i.e. fixed and cleared, samples of this size.

Spherical aberrations induced by refractive index mismatch can be avoided by using immersion lenses designed specifically for the sample medium. Most live imaging is performed in aqueous media and water-dipping lenses, which are designed for glass-free sample preparations, are available in different magnifications. Optimal imaging conditions are achieved when water-dipping lenses are used for both illumination and detection. In multidirectional selective plane illumination microscopy (mSPIM, Fig. 4E), the central unit holds three confocally aligned water-dipping objectives, two for illumination and one for detection (Huisken and Stainier, 2007). mSPIM was developed to overcome two common problems in light-sheet-based imaging techniques: The shadowing in the excitation path due to absorption in the specimen, and the spread of the light-sheet by scattering in the sample. Because of the side-on illumination, light-sheet-based techniques such as conventional SPIM, DSLM, OPFOS and ultramicroscopy suffer from absorption, which results in stripes and shadows along the direction of illumination. These stripes are apparent in many images in the SPIM literature (e.g. Voie et al., 1993; Huisken et al., 2004; Buytaert and Dirckx, 2007; Dodt et al., 2007; Scherz et al., 2008; Keller et al., 2008). In mSPIM, even illumination is achieved by pivoting the light-sheet within the focal plane of the detection optics, thereby illuminating the sample from a range of angles during the camera exposure (Fig. 5; see Movie 1 in the supplementary material). In addition, two opposing objective lenses illuminate the sample from the side (Fig. 4E). However, in contrast to ultramicroscopy, the illumination from the two sides is not simultaneous but sequential; two images are acquired and computationally fused into one. mSPIM has been shown to improve image quality dramatically in living, scattering organisms like zebrafish embryos (Huisken and Stainier, 2007). Fig. 5 illustrates the effect for an 8 hours post fertilization (hpf) and a 32 hpf zebrafish embryo. In mSPIM, stripes and shadows are strongly reduced (Fig. 5C), and both hemispheres of the early embryo are well illuminated. In principle, any light-sheet technique would benefit from such multidirectional illumination.

The arrangement of three objective lenses in mSPIM leaves little space for the sample. In the current implementation with three water-dipping lenses, the space between the lenses is only 6 mm in diameter, which sets an upper limit for the size of the specimen. Light-sheet techniques with only a single objective lens could potentially be used to approach large specimens and to image their surface to a depth defined by the working distance of this objective and unconstrained by additional illumination optics. Recently, a single lens light-sheet technique has been developed for much smaller sample sizes (<20 μm). In highly inclined and laminated optical sheet (HILO) microscopy (Tokunaga et al., 2008) (Fig. 4F), a thin, inclined beam is used to image single molecules in cells. The sample, which is mounted onto a coverslip, is illuminated at an angle just below the angle of total refraction [as used in total internal reflection fluorescence (TIRF) microscopy]. The result is a laser beam that intersects the focal plane at a shallow angle and optically sections the sample. HILO microscopy has been used to study the interaction between single GFP-tagged importin β molecules and nuclear pore complexes. Photo-bleaching was reported to be much lower than in LSCM, and the signal-to-noise ratio was much improved over epifluorescence microscopy. The achievable field of view in HILO microscopy is very limited because the sheet of illumination is tilted and illuminates the focal plane of the detection lens only in a single line. However, the image plane can also be tilted with optics in the detection path as in oblique plane microscopy (OPM), which enables an oblique plane in the specimen to be illuminated and imaged with the same objective lens (Dunsby, 2008).

Instead of a dedicated light-sheet microscope setup, light-sheet illumination can also be realized as an add-on to an existing microscope. In the design shown in Fig. 4G, the excitation light is projected onto the sample by a cap attached to the objective (Wolleschensky, 2008). Such an arrangement would even allow for illumination from more than two sides.

Sample preparation for light-sheet-based microscopy

The sample preparation for light-sheet techniques is very different from the slide preparations used for conventional microscopy. For ultramicroscopy, the fixed sample is immersed in a clearing solution and illuminated and imaged from outside the chamber. For SPIM, mSPIM and DSLM, the live sample is most often immersed in an aqueous medium. In order to control the position of the sample precisely with respect to the light-sheet and the detection lens, large samples like zebrafish or *Drosophila* embryos are embedded in a transparent gel, such as agarose, and held in place from the top by micromotors. Single cells and cysts are generally embedded in hollow agarose cylinders or Matrigel enclosed in a small bag of transparent foil (Keller et al., 2006). The embedded sample is then immersed in an aqueous medium appropriate for the particular sample. In a recent mSPIM implementation in the authors' laboratory, the chamber is connected to a computer-controlled perfusion pump and an in-line heater, which provide temperature-controlled fresh medium. This setup allows for the sample under observation to be heat-shocked or treated with drugs for well-defined time periods. Of course, light-sheet microscopy is not limited to samples immersed in a medium; setups with air lenses can also be employed.

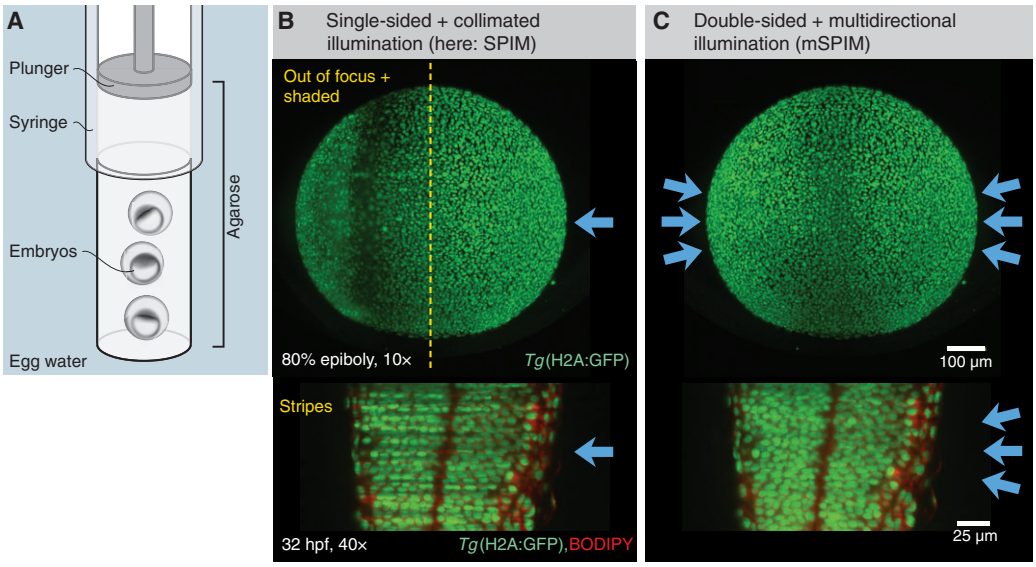

Fig. 5. Comparison of single-sided SPIM and mSPIM. Multidirectional selective plane illumination microscopy (mSPIM) dramatically reduces absorption and scattering artifacts and provides an evenly illuminated focal plane, as demonstrated with zebrafish embryos. Blue arrows indicate direction of illumination. (**A**) Schematic representation of the sample preparation for light-sheet microscopy: multiple zebrafish embryos are embedded in a low melting point agarose cylinder inside a syringe. To image the embryos, the cylinder is partially pushed out of the syringe and dips into the medium-filled chamber (not shown). Three embryos are stacked in the agarose and are sequentially imaged during a time-lapse recording. Shown are early embryos embedded and imaged in their chorion. (**B**) 8 hpf (top) and 32 hpf (bottom) zebrafish embryos imaged using SPIM. The illumination from the right in SPIM does not penetrate the whole embryo at 80% epiboly. The light-sheet gets refracted and renders the left half blurry and patchy. (B, bottom) Stripes are especially apparent at later stages, when pigmentation has occurred, which can block the light-sheet. (**C**) In mSPIM, by contrast, the sample is sequentially illuminated from two sides from a range of angles. The double-sided illumination yields almost even illumination in the early embryo (C, top), and the pivoting light-sheet eliminates most of the stripes and shadows in the late embryo (C, bottom). See Movie 1 in the supplementary material.

A common feature of SPIM, mSPIM and DSLM is the ability to turn the sample. The agarose in which the sample is mounted is therefore usually formed into a cylinder, which provides an unrestricted view from all sides (Fig. 2E). Because of the vertical rotation axis, the sample does not deform when being turned. For many applications, this additional degree of freedom has turned out to be essential to orient the sample precisely (e.g. Scherz et al., 2008). The vertical orientation is also an important prerequisite for multi-view reconstruction, an imaging strategy that, as we discuss below, has attracted extensive research since the more widespread adoption of light-sheet-based microscopy approaches.

Multi-view reconstruction

In multi-view reconstruction (MVR), multiple 3D image stacks are acquired from two or more sides of the same sample. Subsequently, the resulting data stacks are computationally fused into a single dataset. In practice, the acquisition is generally realized by arranging a number of objective lenses around the sample (Swoger et al., 2003) or by imaging the sample at different orientations with a single objective lens, as in SPIM (Huisken et al., 2004). There are two major benefits to MVR: (1) in large or strongly scattering and absorbing tissue, the uniformity of image quality is improved (ideally scaling with the number of views); and (2) in transparent samples and in regions where the datasets overlap, the resolution in images is improved and becomes isotropic (see Glossary in Box 1; for two orthogonal image stacks, the good lateral resolution of one dataset compensates the poor axial resolution of the other dataset). Generally, a combination of both benefits is achieved in most samples. MVR in fluorescence light-sheet microscopy is optional and can be employed when needed. This is in contrast to tomographic techniques, in which a certain number of projections need to be acquired before a 3D dataset can be computed. Whereas MVR is not limited to SPIM, it performs especially well in SPIM setups; owing to their horizontal detection axis, the sample can be turned about a vertical axis with essentially no sample deformation. Also, the high signal-to-noise ratio achieved by SPIM allows the use of further image processing techniques, such as deconvolution, during MVR.

A number of different MVR techniques have been developed. The general goal of all of these algorithms is to extract the ‘most useful’ information from all the datasets and to merge it into a single dataset, replacing the inferior information of other datasets. This idea was first developed for tilted-view microscopy (Shaw et al., 1989) and later formulated for a double-axis fluorescence microscope (Kikuchi et al., 1997). Recently, more refined methods have been presented for multiple imaging axis microscopy (MIAM) (Swoger et al., 2003) and SPIM (Swoger et al., 2007). Ultimately, it is desirable to combine the fusion algorithm with a simultaneously performed deconvolution algorithm for superior results (Verveer et al., 2007). MVR has been used for the 3D reconstruction of medaka embryos (Huisken et al., 2004; Swoger et al., 2007), *Drosophila* embryos (Swoger et al., 2007; Preibisch et al., 2008) and cysts generated with cells of the MDCK kidney cell line (Verveer et al., 2007).

Apart from the combination of multiple views, further image processing and data management tools are useful when using light-sheet microscopy techniques, mainly because of the vast amount of image data that can rapidly be recorded. Software packages like

ImageJ, Matlab and Labview are widely used for image analysis and data processing on small and large scales. Many public domain plugins and scripts can be found for a number of routine image manipulation tasks (http://rsbweb.nih.gov/ij/plugins/, http://www.mathworks.com/matlabcentral/fileexchange/). Because of their high quality (especially good axial resolution, high dynamic range and low noise), SPIM datasets generally do not require common preprocessing routines such as denoising, deconvolution or unmixing. Rather, it is the complexity of the new information from the inside of living embryos that calls for new tools for data segmentation, visualization and navigation. As SPIM data are mostly not only 3D, multi-color and multi-view, but also represent a time sequence, it is especially challenging to extract and illustrate the dynamics that are hidden in these data. A well-executed example of such an analysis is the recent study of the early embryonic development of the zebrafish, in which 1.5 billion pixels per minute were acquired and automated image segmentation and cell tracking were performed on large computer clusters to describe hypoblast formation (Keller et al., 2008). Given that such computing power is not available to many researchers, the establishment of collaborations and infrastructures in which the biology research community has access to microscopy image databases, similar to shared databases from large-scale physics experiments, would be beneficial.

Light-sheet-based microscopy's wide range of applications

Because of its high depth penetration, low bleaching and high acquisition speed, light-sheet microscopy is ideally suited for a number of applications. Primarily, in vivo time-lapse studies constitute a growing field where light-sheet microscopy can perform better than established techniques (e.g. confocal microscopy) owing to its superior speed and low light exposures. Another benefit of SPIM is the ability to image whole biological samples under physiologically relevant conditions. In SPIM, the sample is kept alive at optimal conditions, and the microscope has been 'built around' the sample in its chamber. By contrast, in classical microscopes, a lot of effort is required to include heated chambers and flow cells to keep samples alive. MVR in SPIM is another unique feature that will enable novel in toto imaging studies. The ability to image an entire embryo from different sides is crucial for developmental studies in which cells are tracked over several hours along paths across the entire embryo. However, it has to be taken into account that in light-sheet microscopy, both illumination and detection paths need to be free of obstacles. Hence, more care has to be taken when orienting and embedding samples for light-sheet microscopy than for single lens microscopes. Spherical samples, such as early zebrafish embryos, or ellipsoidal samples, such as *Drosophila* embryos and larvae, can be imaged well from one or more sides. Large tissues, such as mouse brains, in which only a small area on one side is to be imaged, can be difficult to align to allow proper light-sheet illumination and are therefore not suitable for MVR.

Light-sheet microscopes can be built and optimized for a wide range of sample sizes, from single cells to whole embryos. Single cells primarily benefit from the low bleaching; light-sheet based microscopy has helped researchers understand the biophysics of microtubule dynamics and the development of 3D cell cultures (Keller et al., 2006). The study of complex organisms is aided by optical sectioning and by the ability to use live samples; relatively transparent embryos like medaka (Huisken et al., 2004) and zebrafish (Keller et al., 2008) are particularly well suited for in vivo imaging in toto. More opaque embryos, such as those of *Drosophila*, especially benefit from MVR (Swoger et al., 2007). The high acquisition speed of SPIM reduces the recording times significantly when millimeter-sized embryos need to be imaged at high resolution and at short time intervals. Fig. 6 illustrates two examples in which the development of the vascular system in zebrafish was monitored in 3D over time. Image stacks were acquired at time intervals of 5 minutes (Fig. 6B; see Movie 2 in the supplementary material) and 1 minute (Fig. 6C; see Movie 3 in the supplementary material).

The high sensitivity and speed of SPIM also offers a new approach to high-speed heart imaging in medaka and zebrafish (Huisken et al., 2004). Heart development has previously been primarily analyzed using fixed sections, in which the cardiac tissue is often deformed and collapsed. Obviously, the dynamic development and function of the heart can only be analyzed in living tissue. Optical sections of beating zebrafish hearts have

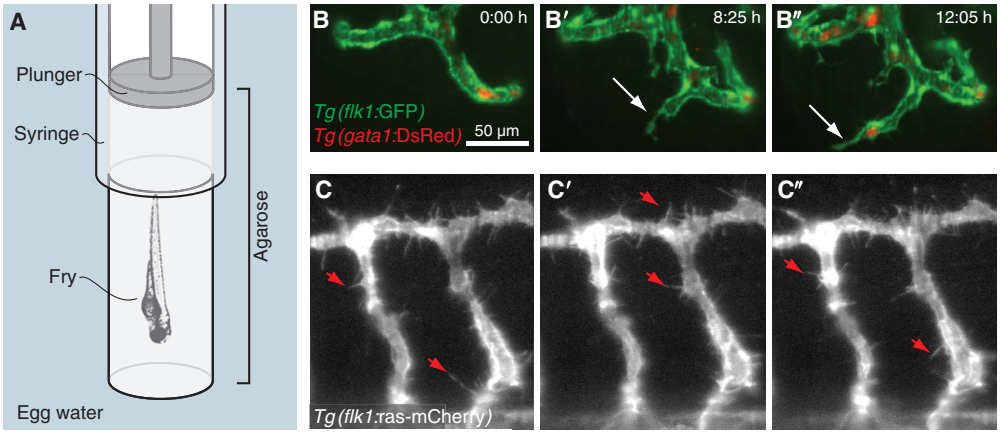

Fig. 6. Vascular endothelial cell dynamics at long and short time scales. Dynamics in cell migration are captured with high-speed SPIM time-lapse recordings. (**A**) Individual or multiple zebrafish larvae are embedded in low melting point agarose. Shown is a single zebrafish larva (Fry) in a vertical orientation, which is ideal for imaging the organs in the trunk and the vasculature in the tail. (**B-B″**) Individual frames from a time-lapse sequence monitoring the sprouting of a vessel (arrow) in the head of a 24 hpf zebrafish. *Tg(flk1:*GFP*)*^{s843} expression labels the endothelial cells and *Tg(gata1:*DsRed*)*^{sd2} expression labels the red blood cells. Shown are maximum intensity projections of a 3D stack. (**C-C″**) Highly dynamic protrusions (arrowheads) in vascular endothelial cells labeled by *Tg(flk1:*ras-mCherry*)*^{s896} expression in a 32 hpf zebrafish. A 3D stack was acquired every minute. Shown are maximum intensity projections captured 10 minutes apart. See Movies 2 and 3 in the supplementary material.

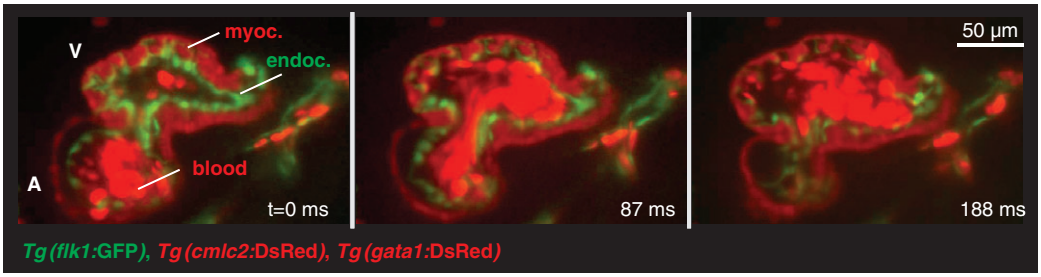

Fig. 7. High-speed recordings of zebrafish heart beats. High-speed mSPIM video sequence of a transgenic fish expressing fluorescent proteins in the endocardium [*Tg(flk1:*GFP*)*^{s843}], myocardium [*Tg(cmlc2:*DsRed*)*^{s879}] and blood [*Tg(gata1:*DsRed*)*^{sd2}]. The movie was recorded at 69 frames per second. Three frames are shown, corresponding to the atrial diastole (left), the atrial systole (middle) and the ventricular diastole (right). A, atrium; V, ventricle; myoc., myocardium; endoc., endocardium. See Movie 4 in the supplementary material.

been collected with commercial confocal laser slit scanning systems at frame rates of up to 150 frames per second (fps) (Liebling et al., 2006). High-speed cameras can be used in light-sheet microscopy to provide similar frame rates (30-200 fps, depending on the frame size). The full frame acquisition in SPIM is free of motion artifacts and more efficient than the line-by-line acquisition of slit scanning microscopes. One promising application for SPIM is therefore the 3D-resolved in vivo cardiac optical mapping during zebrafish heart development. SPIM has played a key role in characterizing the phenotype of a K^+ channel gene (*kcnh2*) mutant by imaging fluctuating Ca^{2+} concentrations in the heart with high spatial and temporal resolution (Arnaout et al., 2007). Another transgenic zebrafish line, which expresses GFP in the endocardium and DsRed in the red blood cells, has been used to study valve morphogenesis. By imaging the atrioventricular (AV) canal in these transgenic fish, AV valve morphogenesis could be investigated at cellular resolution at different developmental stages. SPIM has revealed that what had been previously described as an endocardial cushion actually appears to be a dynamic valve leaflet (Scherz et al., 2008). Fig. 7 and Movie 4 (in the supplementary material) show an example of high-speed cardiac imaging. The transgenic zebrafish line used expresses DsRed in the blood cells and the myocardium and EGFP in the endocardium.

The distinct sample embedding techniques used for light-sheet-based microscopy might seem taxing at first, but this microscopy technique also offers a chance to rethink established protocols and to make the transition from fixed to live imaging, or from 2D to 3D cell and tissue cultures. The embedding medium and the buffer can also be used to match the refractive index of samples that normally develop in air. Fig. 8 (see Movie 5 in the supplementary material) shows an example in which a *Drosophila* pupa was imaged embedded in agarose. The light-sheet penetrates the pupal case in the aqueous environment much better than in air and excites fluorescence in the labeled neurons. A glass capillary is introduced to provide the pupa with air during the time-lapse experiment, which had a duration of 10 hours. Sum projections of 3D stacks document the process of dendrite pruning (Kuo et al., 2005). At the end of the larval stage, the mature fly is able to hatch and escape through the capillary.

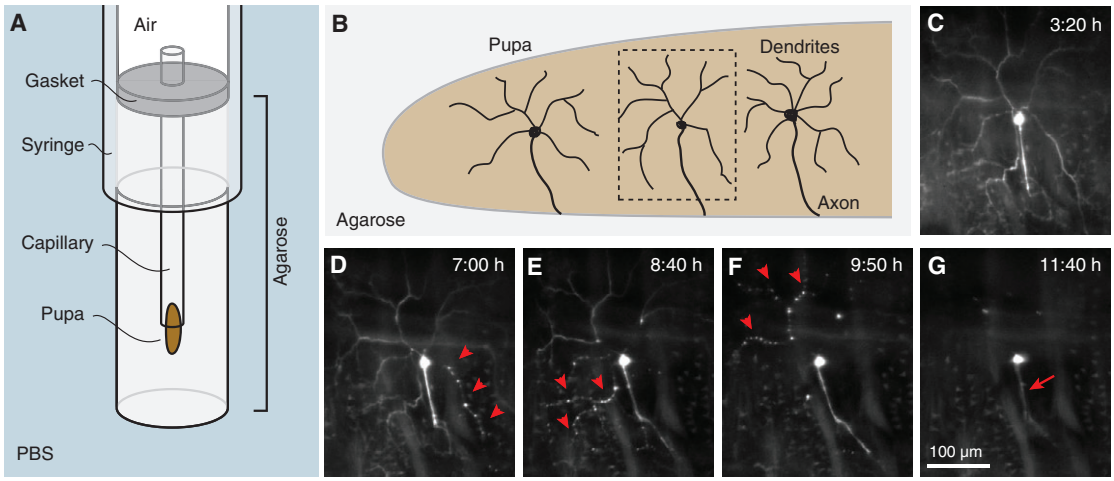

Fig. 8. Dendrite pruning in class IV da neurons in *Drosophila*. *Drosophila* pupae can be imaged in SPIM over many hours using the depicted embedding. (**A**) A *Drosophila* pupa is partially inserted into a glass capillary and embedded in agarose. The high refractive index medium facilitates imaging structures inside the pupal case, while the glass capillary provides enough air for the pupa to survive and space to hatch. (**B**) Schematic of the abdomen of an early *Drosophila* pupa, showing the position and the dendritic fields of dorsal class IV da (ddaC) neurons. (**C-G**) Dendrite pruning of one ddaC neuron (outlined in B) during the course of almost 10 hours; shown are timepoints between 3 hours and 20 minutes and 11 hours and 40 minutes after pupal formation. Arrowheads point to detaching and degenerating dendrites. Only the axon (arrow) remains in G. See Movie 5 in the supplementary material.

Conclusions

Fluorescence light-sheet microscopy features a number of advantages over established microscopy techniques such as epifluorescence microscopy and LSCM. The most prominent benefit is the reduced photo-toxicity, clearly a feature that every in vivo application benefits from. Combined with the rapid acquisition speed, it makes light-sheet microscopy the ideal microscopy technique for extended time-lapse imaging. Fast-moving objects can be tracked in single-plane movies, and 3D volumes can be rapidly sectioned at high image rates with high sensitivity and an unprecedented dynamic range. Light-sheet microscopy is easily upgradeable and will therefore directly benefit from the latest camera technology. Without doubt, cameras with higher resolution, more pixels, better sensitivity and faster data read-out will become available and will be compatible with, and further enhance, light-sheet microscopy.

SPIM has demonstrated that it is possible to deliver optical sectioning deep inside extended objects such as millimeter-sized embryos. The inevitable loss in image quality with increased depth is usually associated with a broadening of the light-sheet and a loss in sectioning. Scattering widens and absorption attenuates the light-sheet as it penetrates dense tissue. The thickness of the light-sheet (and of the optical section) might increase with depth from ~5 μm to 10-15 μm in a millimeter-sized sample. The fluorescence intensity, however, is almost constant throughout the depth of an image stack. This is in contrast to LSCM, in which the signal is simply lost at a certain depth. In SPIM, the attenuation of the light-sheet along its path can be compensated by multidirectional illumination, as exemplified by mSPIM. The inherent penetration depth of SPIM can be further increased severalfold by acquiring multiple data stacks and by merging them computationally. Multi-view fusion is currently unique to SPIM and is an indispensible tool for any object larger than the penetration depth of a single stack. In addition, overlapping datasets can be processed to yield an increase and an isotropy of resolution that is not met by any other single-lens fluorescence microscopy technique. In the future, new algorithms will become more efficient at handling the enormous amounts of data that are acquired in multi-view, multi-color, high-resolution and high-speed microscopy. Again, the field will benefit from the latest technological developments, with more affordable and more powerful computers coming to market.

SPIM and other microscopy techniques compatible with whole organs and live embryos have opened new dimensions in developmental biology; the development of certain organs can be followed in the living animal at single-cell resolution; the growth of primitive cell clusters can be studied in 3D as they form cysts and tubes; and single cells can be tracked as they interact in a matrix free from confining glass surfaces. However, the newly gained experimental opportunities come at a small but real cost: the requirement to rethink established sample preparation techniques and to develop new strategies for live imaging. This area is still in its infancy, but new experimental techniques will emerge as more scientists become aware of the importance and usefulness of 3D sample preparation.

Despite the variety of names and acronyms for light-sheet based microscopes, the multitude of recent developments clearly shows how important light-sheet microscopy techniques are becoming for modern developmental biology. They are a key technology for in toto fluorescence imaging and high-speed image acquisition in live organisms. At the same time, the variety of light-sheet-based microscopy implementations shows that the universal concept of light-sheet illumination can be adapted to a number of different applications, with samples ranging from single cells to whole mouse embryos. It also demonstrates that there is still room for future developments. Novel and customized optical elements will become available in the future to form thinner and more uniform light-sheets, and new objective lenses will provide high NAs at large working distances. In summary, the concept of light-sheet-based microscopy is powerful and straightforward, the implementations are manifold and easily customized to meet individual needs, and the number of applications is growing.

We thank Jim Swoger, Stephanie Woo, Kurt Thorn and Geoffrey Lambright for critical comments on the manuscript; and Sebastian Rumpf and Yuh Nung Jan for providing the *Drosophila* sample. J.H. is supported by a Human Frontier Science Program (HFSP) fellowship. Support for the SPIM work in our lab comes from grants from the NIH (NHLBI and NIDDK), the Sandler Family Foundation and the Packard Foundation to D.Y.R.S. Deposited in PMC for release after 12 months.

Supplementary material

Supplementary material for this article is available at
http://dev.biologists.org/cgi/content/full/136/12/1963/DC1

References

Arnaout, R., Ferrer, T., Huisken, J., Spitzer, K., Stainier, D. Y. R., Tristani-Firouzi, M. and Chi, N. C. (2007). Zebrafish model for human long QT syndrome. *Proc. Natl. Acad. Sci. USA* **104**, 11316-11321.

Becker, K., Jährling, N., Kramer, E. R., Schnorrer, F. and Dodt, H.-U. (2008). Ultramicroscopy: 3D reconstruction of large microscopical specimens. *J. Biophotonics* **1**, 36-42.

Breuninger, T., Greger, K. and Stelzer, E. H. K. (2007). Lateral modulation boosts image quality in single plane illumination fluorescence microscopy. *Opt. Lett.* **32**, 1938-1940.

Buytaert, J. A. N. and Dirckx, J. J. J. (2007). Design and quantitative resolution measurements of an optical virtual sectioning three-dimensional imaging technique for biomedical specimens, featuring two-micrometer slicing resolution. *J. Biomed. Opt.* **12**, 014039.

Denk, W. and Horstmann, H. (2004). Serial block-face scanning electron microscopy to reconstruct three-dimensional tissue nanostructure. *PLoS Biol.* **2**, e329.

Dodt, H. U., Leischner, U., Schierloh, A., Jährling, N., Mauch, C., Deininger, K., Deussing, J. M., Eder, M., Zieglgänsberger, W. and Becker, K. (2007). Ultramicroscopy: three-dimensional visualization of neuronal networks in the whole mouse brain. *Nat. Methods* **4**, 331-336.

Dunsby, C. (2008). Optically sectioned imaging by oblique plane microscopy. *Opt. Express* **16**, 20306-20316.

Engelbrecht, C. J. and Stelzer, E. H. K. (2006). Resolution enhancement in a light-sheet-based microscope (SPIM). *Opt. Lett.* **31**, 1477-1479.

Engelbrecht, C. J., Greger, K., Reynaud, E. G., Krzic, U., Colombelli, J. and Stelzer, E. H. K. (2007). Three-dimensional laser microsurgery in light-sheet based microscopy (SPIM). *Opt. Express* **15**, 6420-6430.

Ewald, A. J., McBride, H., Reddington, M., Fraser, S. E. and Kerschmann, R. (2002). Surface imaging microscopy, an automated method for visualizing whole embryo samples in three dimensions at high resolution. *Dev. Dyn.* **225**, 369-375.

Fuchs, E., Jaffe, J. S., Long, R. A. and Azam, F. (2002). Thin laser light sheet microscope for microbial oceanography. *Opt. Express* **10**, 145-154.

Haas, P. and Gilmour, D. (2006). Chemokine signaling mediates self-organizing tissue migration in the zebrafish lateral line. *Dev. Cell* **10**, 673-680.

Hell, S. (2007). Far-field optical nanoscopy. *Science* **316**, 1153-1158.

Helmchen, F. and Denk, W. (2005). Deep tissue two-photon microscopy. *Nat. Methods* **2**, 932-940.

Holekamp, T. F., Turaga, D. and Holy, T. E. (2008). Fast three-dimensional fluorescence imaging of activity in neural populations by objective-coupled planar illumination microscopy. *Neuron* **57**, 661-672.

Huber, D., Keller, M. and Robert, D. (2001). 3D light scanning macrography. *J. Microsc.* **203**, 208-213.

Huisken, J. and Stainier, D. Y. R. (2007). Even fluorescence excitation by multi-directional selective plane illumination microscopy (mSPIM). *Opt. Lett.* **32**, 2608-2610.

Huisken, J., Swoger, J., Del Bene, F., Wittbrodt, J. and Stelzer, E. H. K. (2004). Optical sectioning deep inside live embryos by selective plane illumination microscopy. *Science* **305**, 1007-1009.

Kamei, M. and Weinstein, B. M. (2005). Long-term time-lapse fluorescence imaging of developing zebrafish. *Zebrafish* **2**, 113-123.

Keller, P. J., Pampaloni, F. and Stelzer, E. H. K. (2006). Life sciences require the third dimension. *Curr. Opin. Cell Biol.* **18**, 117-124.

Keller, P. J., Schmidt, A. D., Wittbrodt, J. and Stelzer, E. H. K. (2008).

Reconstruction of zebrafish early embryonic development by scanned light sheet microscopy. *Science* **322**, 1065-1069.
Kikuchi, S., Sonobe, K., Mashiko, S., Hiraoka, Y. and Ohyama, N. (1997). Three-dimensional image reconstruction for biological micro-specimens using a double-axis fluorescence microscope. *Opt. Commun.* **138**, 21-26.
Kuo, C. T., Jan, L. Y. and Jan, Y. N. (2005). Dendrite-specific remodeling of Drosophila sensoryneurons requires matrix metalloproteases, ubiquitin-proteasome, and ecdysone signaling. *Proc. Natl. Acad. Sci. USA* **102**, 15230-15235.
Liebling, M., Forouhar, A. S., Wolleschensky, R., Zimmermann, B., Ankerhold, R., Fraser, S. E., Gharib, M. and Dickinson, M. E. (2006). Rapid three-dimensional imaging and analysis of the beating embryonic heart reveals functional changes during development. *Dev. Dyn.* **235**, 2940-2948.
McLachlan, D., Jr (1968). Microscope. *US Patent* 3398634.
McNally, J. G., Karpova, T., Cooper, J. and Conchello, J. A. (1999). Three-dimensional imaging by deconvolution microscopy. *Methods* **19**, 373-385.
Pawley, J. (2006). *Handbook of Confocal Microscopy.* New York: Springer.
Preibisch, S., Rohlfing, T., Hasak, M. P. and Tomancak, P. (2008). Mosaicing of single plane illumination microscopy images using groupwise registration and fast content-based image fusion. *Proc. SPIE* **6914**, 69140E.
Rembold, M., Loosli, F., Adams, R. J. and Wittbrodt, J. (2006). Individual cell migration serves as the driving force for optic vesicle evagination. *Science* **313**, 1130-1134.
Ritter, J. G., Veith, R., Siebrasse, J.-P. and Kubitscheck, U. (2008). High-contrast single-particle tracking by selective focal plane illumination microscopy. *Opt. Express* **16**, 7142-7152.
Scherz, P. J., Huisken, J., Sahai-Hernandez, P. and Stainier, D. Y. R. (2008). High-speed imaging of developing heart valves reveals interplay of morphogenesis and function. *Development* **135**, 1179-1187.
Sharpe, J., Ahlgren, U., Perry, P., Hill, B., Ross, A., Hecksher-Sørensen, J., Baldock, R. and Davidson, D. (2002). Optical projection tomography as a tool for 3D microscopy and gene expression studies. *Science* **296**, 541-545.
Shaw, P. J., Agard, D. A., Hiraoka, Y. and Sedat, J. W. (1989). Tilted view reconstruction in optical microscopy. Three-dimensional reconstruction of *Drosophila melanogaster* embryo nuclei. *Biophys. J.* **55**, 101-110.
Siedentopf, H. and Zsigmondy, R. (1902). Über Sichtbarmachung und Größenbestimmung ultramikoskopischer Teilchen, mit besonderer Anwendung auf Goldrubingläser. *Ann. Phys.* **10**, 1-39.
Simon, W. (1965). Photomicrography of deep fields. *Rev. Sci. Instrum.* **36**, 1654-1655.
Swoger, J., Huisken, J. and Stelzer, E. H. K. (2003). Multiple imaging axis microscopy improves resolution for thick-sample applications. *Opt. Lett.* **28**, 1654-1656.
Swoger, J., Verveer, P., Greger, K., Huisken, J. and Stelzer, E. H. K. (2007). Multi-view image fusion improves resolution in three-dimensional microscopy. *Opt. Express* **15**, 8029-8042.
Tokunaga, M., Imamoto, N. and Sakata-Sogawa, K. (2008). Highly inclined thin illumination enables clear single-molecule imaging in cells. *Nat. Methods* **5**, 159-161.
Turaga, D. and Holy, T. E. (2008). Miniaturization and defocus correction for objective-coupled planar illumination microscopy. *Opt. Lett.* **33**, 2302-2304.
Verveer, P. J., Swoger, J., Pampaloni, F., Greger, K., Marcello, M. and Stelzer, E. H. K. (2007). High-resolution three-dimensional imaging of large specimens with light sheet-based microscopy. *Nat. Methods* **4**, 311-313.
Voie, A. H. (2002). Imaging the intact guinea pig tympanic bulla by orthogonal-plane fluorescence optical sectioning microscopy. *Hear. Res.* **171**, 119-128.
Voie, A. H., Burns, D. H. and Spelman, F. A. (1993). Orthogonal-plane fluorescence optical sectioning: three-dimensional imaging of macroscopic biological specimens. *J. Microsc.* **170**, 229-236.
Weninger, W., Geyer, S., Mohun, T., Rasskin-Gutman, D., Matsui, T., Ribeiro, I., Costa Lda, F., Izpisúa-Belmonte, J. C. and Müller, G. B. (2006). High-resolution episcopic microscopy: a rapid technique for high detailed 3D analysis of gene activity in the context of tissue architecture and morphology. *Anat. Embryol.* **211**, 213-221.
Wolleschensky, R. (2008). Arrangement for microscopic observation and/or detection in a light scanning microscope with line scanning and use. *US Patent Appl.* US 20080030850.
Zampol, P. (1960). Method of Photography. *US Patent* 2928734.